

Clean recoil implantation of the $^{100}\text{Pd/Rh}$ TDPAC probe using a solenoidal separator

A. A. Abiona¹, W.J. Kemp¹, E. Williams², H. Timmers¹

¹School of Physical, Environmental and Mathematical Sciences, The University of New South Wales Canberra, PO Box 7916, Canberra BC 2610, Australia.

²Department of Nuclear Physics, RSPE, Australian National University, ACT 0200, Australia.

Abstract. The synthesis and recoil implantation of the $^{100}\text{Pd/Rh}$ probe for time differential perturbed angular correlation (TDPAC) spectroscopy using the solenoidal reaction product separator SOLITAIRE has been demonstrated for the first time. The separator suppresses the co-implantation of the intense flux of elastically scattered projectile ions that can affect results obtained with the hyperfine interactions technique. Using three different fusion evaporation reactions, the solenoid field was optimised at 4.5 T to achieve a concentrated, circular focus of evaporation residue ions with a lateral FWHM of 20 mm. Employing the reaction $^{92}\text{Zr}(^{12}\text{C},4n)^{100}\text{Pd}$ several samples have been recoil-implanted with the $^{100}\text{Pd/Rh}$ probe. Gamma-ray spectroscopy of a silver sample and a TDPAC measurement on zinc confirm that the new preparation technique is effective. The ratio function measured with TDPAC of an undoped germanium sample may indicate that palladium-defect pairs are absent when implanting with SOLITAIRE. However, a direct comparison with TDPAC results for germanium samples prepared with conventional recoil implantation, which does not suppress the flux of elastics, does not support this assertion.

1 Introduction

With the aim of developing smaller devices, germanium promises to be an alternative to silicon in complementary-metal-oxide-semiconductor technology since it can be annealed at lower temperatures. Palladium is well suited to induce the crystallisation of germanium at such low temperatures. It is, however, not clear how residual Pd-atoms are integrated in the germanium lattice following crystallisation [1-4]. The presence of residual palladium atoms and their lattice and defect interactions can affect the electronic properties of the material. With Time Differential Perturbed Angular Correlation (TDPAC) spectroscopy using the probe $^{100}\text{Pd/Rh}$, the local lattice environment of palladium atoms in crystalline germanium can be studied at the atomic scale.

Previous TDPAC spectroscopy, following the synthesis of the $^{100}\text{Pd/Rh}$ probe via a fusion evaporation reaction and recoil implantation into germanium, has identified that after annealing of beam-induced lattice damage a non-zero electric field gradient (EFG) exists at the probe location [5,6]. This EFG may be caused by the pairing of the palladium atom with a neighbouring defect, which is most likely a vacancy. Such a pairing is illustrated in Fig. 1 assuming that the pair is oriented in the $\langle 111 \rangle$ direction as suggested by other work [6].

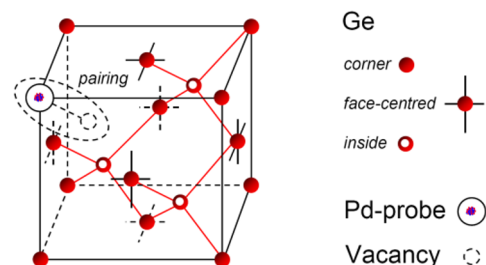


Fig. 1. Illustration of a palladium-vacancy pair (dashed ellipse), oriented in the $\langle 111 \rangle$ direction inside the germanium lattice. [All figures in this paper are displayed in colour in the online version.]

During recoil implantation, the germanium samples are placed at forward angles just outside the ^{12}C projectile beam, where the evaporation residue yield is largest. In this location, however, the samples are exposed to projectiles that are elastically scattered in the ^{92}Zr target [7]. The scattering yield incident on the samples is several orders of magnitude larger than the yield of recoiling evaporation residues. Since the energy of the scattered ^{12}C projectiles is much larger, and their atomic number smaller, than that of the recoiling probe nuclei, the ^{12}C ions implant much deeper inside the

germanium, however, they pass through the region of probe implantation. The lattice damage associated with this passage may increase the number of vacancies available and could aid in the observed formation of palladium-vacancy pairs.

In order to investigate this possibility and also to demonstrate an advanced recoil-implantation technique that fully avoids the intense co-implantation of scattered projectiles, experiments have been performed using the novel 6.5 Tesla superconducting solenoidal separator SOLITAIRE, developed at the Australian National University [8]. This paper presents the results of these experiments and discusses the first TDPAC measurements performed with this advanced sample preparation technique.

2 Experimental Details

2.1 $^{100}\text{Pd}/\text{Rh}$ Synthesis and Implantation

The experiments were performed with the 14UD Pelletron accelerator at the Australian National University. In order to optimize the recoil implantation of the probe using SOLITAIRE, the fusion evaporation reactions $^{76}\text{Ge}(^{29}\text{Si}, 5n)$, $^{92}\text{Zr}(^{13}\text{C}, 5n)$ and $^{92}\text{Zr}(^{12}\text{C}, 4n)$ were all explored at energies for which statistical model calculations predict a maximum yield for the probe. Since the reactions combine different projectile and target nuclei, momentum transfer to the evaporation residues differs and transport through the separator may vary.

Recoil implantation of $^{100}\text{Pd}/\text{Rh}$ into several specimens, including a zinc foil, a piece of silver and a non-doped crystalline germanium sample, was then performed using the $^{92}\text{Zr}(^{12}\text{C}, 4n)$ reaction. The beam energy was 70 MeV. The electrical beam current was kept at 1 μA . The implantation time was 12 hours. The flux of scattered projectile ions was suppressed using SOLITAIRE.

A self-supporting 1 μm thick zirconium target was used. In SOLITAIRE the target is in a low-pressure helium environment (0.5 mbar) that aids in dissipating heat from the target. The target was intact after the implantation. However, pin-holes were apparent. The efficiency of the synthesis may be improved by employing several targets and moving them through the beam. For more details on the solenoidal separator, see [9].

In a separate experiment, using the original recoil implantation setup [7] without suppression of scattered projectiles, the $^{100}\text{Pd}/\text{Rh}$ probe was produced via the same reaction and with the same beam current. The target holder was cooled externally and the implantation time was 20 h.

2.2 TDPAC Spectrometry

The nucleus ^{100}Pd decays with a half-life of $t_{1/2} = 3.6$ d to excited states of ^{100}Rh . In ^{100}Rh a $1^+ - 2^+ - 1^-$ level sequence is connected via an 84–75 keV γ - γ cascade. The intermediate 2^+ -state has a quadrupole moment of $Q = 0.076(2)$ b and interacts with the electric field gradient at the probe location inside the sample.

Three TDPAC spectrometers were used. Two employ four BaF_2 detectors and the third uses four $\text{NaI}(\text{Tl})$ detectors. All spectrometers were set up in the conventional planar geometry with detectors at 90° angles. Detected 84-keV and 75-keV γ -rays provided start and stop signals to a time-to-analogue converter. The coincidence time distributions of these two γ -rays were recorded for all detector combinations using NIM-standard electronics [10]. After correction for statistical background events, the distributions for detectors at 90° and those for detectors at 180° were averaged, thus compensating for differences in detection solid angle and detector efficiency. Finally, using the usual prescription, the ratio functions $R(t)$ were extracted from the data. This is described in details in Ref. [10, 11].

3 Results and Discussions

Figure 2 shows a schematic of the superconducting solenoid SOLITAIRE that illustrates the trajectories of the ^{100}Pd evaporation residues and those of the elastically scattered projectiles. The beam is stopped before the solenoid in a Faraday cup. Elastically scattered projectiles are stopped at blocking discs inside the solenoid. This suppresses the elastic scattering flux almost completely. Any residual scattering flux due to multiple scattering or caused by edge scattering effects has a different focal point than the evaporation residues and will thus mostly also not co-implant.

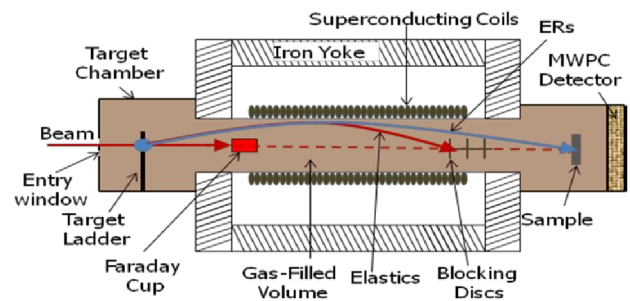


Fig. 2. Illustration of the separation of evaporation residues ^{100}Pd (blue) from elastically scattered projectiles (red) in the superconducting solenoid SOLITAIRE. The schematic is an axial cross-section of the solenoid. The He gas is shown by the orange shading.

In order to concentrate and focus the ^{100}Pd evaporation residues onto the samples that are placed on axis behind the solenoid, the magnetic field needs to be chosen correctly. This choice depends on the reaction kinematics and the average ion charge state of the residues as induced by scattering in the low-pressure helium gas inside the solenoid. Using ^{29}Si -, ^{13}C - and ^{12}C -induced fusion evaporation reactions to synthesize ^{100}Pd , the transport and focusing of this evaporation residue flux with SOLITAIRE has been studied in detail. Residues and elastic scattering were detected behind SOLITAIRE using a position-sensitive multi-wire proportional counter.

The x - y positions of the residues on a plane perpendicularly intersecting the solenoidal axis have been determined as a function of magnetic field strength. It has been confirmed that the scattering flux is separated in space from the flux of residues. As expected, the focusing is symmetric about the solenoidal axis. Figure 3 shows the FWHM determined for the circular x - y distribution of the evaporation residues in the detector as a function of solenoidal field. An optimum image spot with a FWHM of about 20 mm can be achieved at the detector position for a field of 4.5 T. It was found that the transport and focusing of SOLITAIRE is very similar for all three reactions studied.

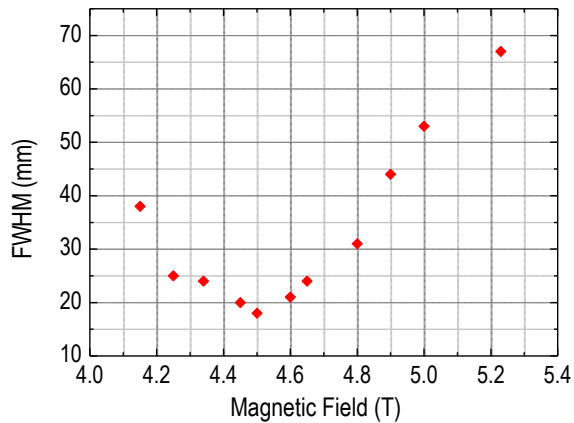


Fig. 3. FWHM of the image spot for evaporation residues from the $^{13}\text{C} + ^{92}\text{Zr}$ system for different solenoidal fields, indicating optimum focusing near 4.5 T.

Since the ^{12}C beam results in the lowest energy residues, and thus the shallowest implantation of the $^{100}\text{Pd/Rh}$ probe, the ^{12}C -induced reaction was selected for the first probe implantation with SOLITAIRE. Figure 4 shows a γ -ray spectrum for the silver sample following recoil implantation with SOLITAIRE. The two γ -ray transitions in ^{100}Rh that are important for TDPAC are identified in the figure and confirm the success of the preparation.

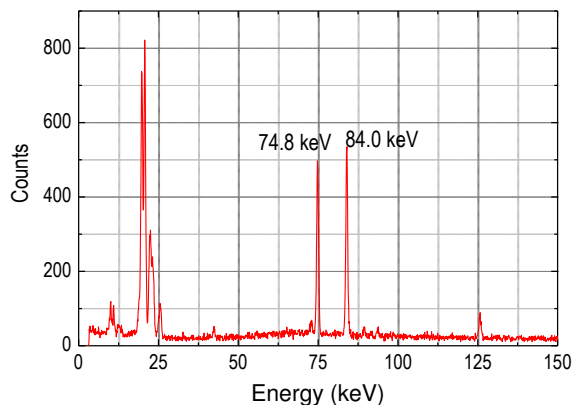


Fig. 4. Gamma-ray spectroscopy confirms the successful implantation of the TDPAC probe $^{100}\text{Pd/Rh}$ while using the capability of SOLITAIRE to suppress the co-implantation of scattered projectiles.

Figure 5 shows the ratio function $R(t)$ as measured with TDPAC for zinc following probe implantation with SOLITAIRE. The data shows the characteristic modulation for the integration of the probe into a polycrystalline sample with hexagonal lattice structure. The fit is in good agreement indicating that most $^{100}\text{Pd/Rh}$ probes have been integrated substitutionally. It may be noted that no annealing was required to achieve such a high degree of integration. This may be because lattice damage in the zinc was kept at a minimum due to the suppression of any co-implantation of elastically scattered projectiles.

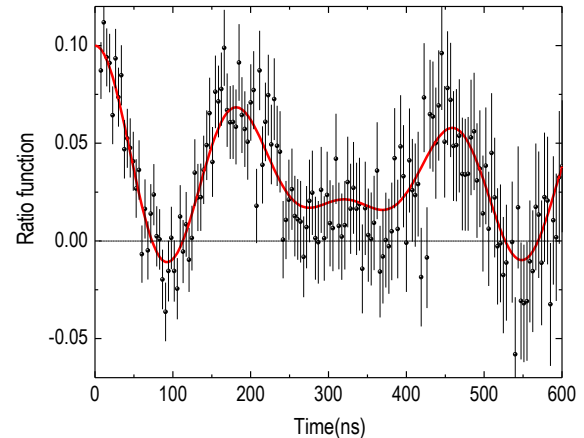


Fig. 5. TDPAC Ratio function $R(t)$ as measured for zinc and a fit (red).

A sample from a non-doped Czochralski-grown (111) germanium wafer was also implanted. Following annealing at 540 °C in flowing nitrogen gas, the specimen was measured with TDPAC with the surface normal of the sample pointing at one of the detectors. The measured ratio function $R(t)$ is shown in Figure 6.

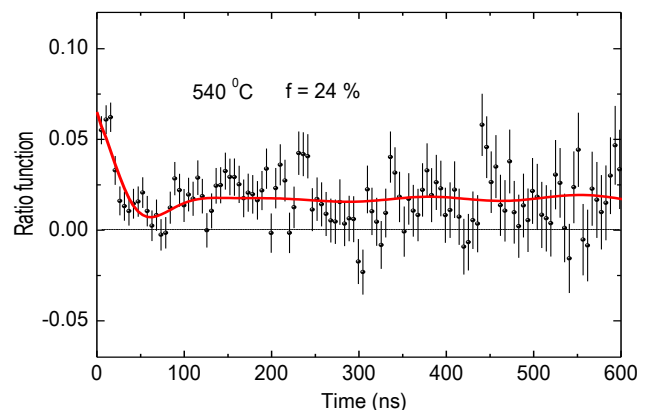


Fig. 6. Measured TDPAC ratio function $R(t)$ and fit for $^{100}\text{Pd/Rh}$ in a non-doped germanium specimen following recoil implantation with SOLITAIRE and annealing at 540 °C.

The annealing temperature was chosen based on previous results, which indicate that the fraction of the palladium-defect pairing in germanium is largest after

annealing at 500 °C [5]. However, it is evident from the data that the measured ratio function is strongly damped, implying that, in this case, only a small fraction of probes, if any, are paired. Furthermore, the damping of the data suggests the presence of several different types of probe environments. This was previously observed following annealing at 700 °C [5]. Since the previous measurements were based on recoil implantations without the suppression of elastic scattering into the specimen, one may speculate that the scattering damage of the lattice is an important precursor for the creation of palladium-defect pairs.

In order to test this hypothesis, the results may be compared with a recent recoil implantation of the probe using the original setup that does not suppress elastic scattering. In this case, the sample is gallium-doped germanium. Following recoil implantation the sample sequentially annealed for 30 min in flowing nitrogen at the temperatures of 300 °C, 350 °C and 540 °C. After each annealing TDPAC spectroscopy was performed. The measured ratio functions and fits are shown in Fig. 7.

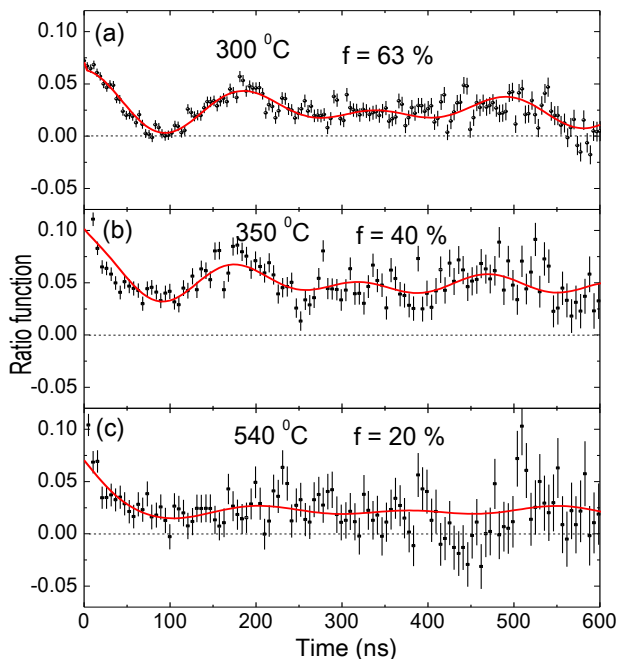


Fig. 7. Measured TDPAC ratio functions $R(t)$ for $^{100}\text{Pd/Rh}$ in a Ga-doped germanium sample following recoil implantation without the suppression of the elastic scattering flux. The sample was annealed at the indicated temperatures before TDPAC. Fits are also shown and the probe fraction f associated with the palladium-defect pair is indicated.

The modulation patterns of the three ratio functions in the figure are similar, with an associated quadrupole coupling constant of $\nu_Q = 8.4$ (2) Mrad/sec. The data consistently show the first minimum and maximum at about $t = 100$ ns and $t = 200$ ns respectively. This is similar to what has been observed previously for $^{100}\text{Pd/Rh}$ in germanium [5,6]. As the annealing temperature increases, the amplitude of the modulation is reduced. This can be understood as a reduction in the fraction f of palladium-defect pairs as the annealing temperature

increases. The fits suggest fractions of (a) 63 %, (b) 40 % and (c) 20 %, respectively.

Importantly, the largest fraction occurs at a temperature that is 200 degrees lower than previously observed for non-doped germanium [5]. The lower temperature may be caused by differences in the annealing procedures applied previously.

The ratio function measured after annealing at 540 °C is not unlike that measured following recoil implantation with SOLITAIRE after annealing at the same temperature. However, counting statistics are poor, so that a conclusive statement on the role of lattice damage in the formation of palladium-defect pairs due to elastic scattering into the sample is not possible.

4. Summary and Conclusions

The unique capabilities of the superconducting solenoidal separator of evaporation residues SOLITAIRE have been applied to the preparation of samples for time differential perturbed angular correlation spectroscopy. It has been demonstrated that samples can be prepared cleanly with a relevant probe while the unwanted intense flux of scattered projectiles is suppressed. For the recoil implantation of the probe $^{100}\text{Pd/Rh}$ the solenoidal field required was found to be largely independent of the projectile-target combination used. An optimum field for the recoil implantation of $^{100}\text{Pd/Rh}$ probe is 4.5 T, which results in a 20 mm wide focal image. Following the implantation γ -ray spectra for the samples showed the characteristic lines of the $^{100}\text{Pd/Rh}$ probe. TDPAC spectroscopy of $^{100}\text{Pd/Rh}$ in zinc has reproduced the well-known ratio function for such a polycrystalline sample with hexagonal lattice structure.

For an undoped germanium sample a strongly damped ratio function has been measured after annealing at 540°C. This may imply the need for elastic scattering co-implantation in the formation of palladium vacancy pairs in germanium. However, comparison with the ratio function for a similar sample, prepared *without* the use of SOLITAIRE, shows good agreement, so this assertion is not supported.

References

1. P. Jin-Hong, PhD-Dissertation, Stanford University (2009).
2. P. Jin-Hong *et al.*, IEEE International Electron Devices Meeting (IEDM), Technical Digest, (San Francisco) p 389.
3. C. O. Chui *et al.*, *IEDM Tech. Dig.* **17**, 437 (2002).
4. S. Gaudet *et al.*, *J. Vac. Sci. Tech. A* **24**, 474 (2006).
5. H. Timmers *et al.*, *Hyperfine Interactions* **197**, 159 (2010).
6. A. A. Abiona *et al.*, 35th Annual Condens. Matter & Mat. Meeting, Wagga-Wagga, Australia (2011).
7. E. Bezakova, Ph.D. thesis, Australian National University, Canberra (1998).
8. M.D. Rodriguez *et al.*, *Nucl. Instr. and Meth. A* **614** 119 (2010).
9. D.J. Hinde *et al.*, these proceedings.
10. G. Schatz and A. Weidinger, *Nuclear Condensed Matter Physics* (New York: Wiley) (1996).
11. H. Frauenfelder and R. M. Steffen, *α -, β - and γ -ray spectroscopy* ed Siegbahn K (Amsterdam: North-Holland) (1965).